

Stannaborate Transition Metal Chemistry: Ligand Properties, Reactivity, and Density Functional Theory Calculations of Platinum and Palladium Complexes

Thiemo Marx,^[a] Lars Wesemann,^{*[a]} Stefanie Dehnen,^[b] and Ingo Pantenburg^[a]

Dedicated to Professor Hansgeorg Schnöckel on the occasion of his 60th birthday

Abstract: Three stannaborate complexes of platinum(II) and a novel stannoborate palladium(II) derivative have been prepared in excellent yield. The tin transition metal bond is formed through nucleophilic substitution and the resulting complexes [Bu₃MeN][*trans*-{(Et₃P)₂Pt(SnB₁₁H₁₁)H}] (6), [*trans*-{(Et₃P)₂Pt(SnB₁₁H₁₁)(CN*t*Bu)}] (7), [Bu₃MeN]₂[*trans*-{(Et₃P)₂Pt(SnB₁₁H₁₁)₂-(CN*t*Bu)}] (8), and [Bu₃MeN][(dppe)-Pd(SnB₁₁H₁₁)Me] (12) (dppe = 1,2-bis-

(diphenylphosphanyl)ethane) were characterized by NMR spectroscopy and elemental analysis. In the cases of the zwitterion 7, the pentacoordinated complex 9, the palladium salt 12 and [(triphos)Pt(SnB₁₁H₁₁)] (10) (triphos = 1,1,1-tris(diphenylphosphanylmethyl)-

Keywords: cluster compounds · density functional calculations · platinum · tin · zwitterions

ethane), their solid-state structures are determined by X-ray crystal structure analyses. The *trans* influence of the [SnB₁₁H₁₁] ligand is evaluated from the results of the IR spectroscopy and X-ray crystallographic structures of complexes 6, 7, and 12. The dipole moment of the zwitterion 7 is calculated by density functional theory (DFT) methods. The alignment of the dipole moments of the polar molecules 7 and 12 in the solid state is discussed.

Introduction

Transition metal tin chemistry has been a field of active research for more than thirty years and is the topic of several review articles.^[1] Transition metal tin bonds are known for almost every transition metal and a variety of synthetic routes to these complexes have been established.^[2] This chemistry is dominated by anionic SnX₃ (X = Cl, Br) and SnR₃ (R = alkyl, aryl) ligands. In the case of alkyl- or aryl-substituted tin derivatives, nucleophilic substitution between either Ph₃SnLi and a transition metal halide or Me₃SnCl and a nucleophilic transition metal complex is the easiest method of preparation. Insertion of the stannylenes (SnX₂) into a metal–metal,

metal–halogen, metal–hydride, or metal–carbon bond is another synthetic pathway to the formation of transition metal tin bonds.^[3] Insertion of SnCl₂ into Pt–Cl bonds has been extensively studied because some products can act as catalysts for homogeneous hydrogenation, isomerization, or hydroformylation of alkenes.^[4] Solutions of chloroplatinic acid and stannous chloride reduce ethylene and acetylene quantitatively at room temperature and atmospheric pressure of hydrogen.^[5] The remarkable *trans* influence of the SnCl₃ ligand and the lability of the ligand itself is thought to play an important role in these catalytic reactions. However, the mechanism of the tin interaction is not fully understood. Asymmetric hydroformylations of alkenes with platinum–phosphane complexes are also carried out with SnCl₂ or SnF₂ as the cocatalyst.^[6, 7]

We found that stanna-*closo*-dodecaborate [SnB₁₁H₁₁]²⁻ can coordinate to transition metal centers.^[8] The synthesis of the ligand is straightforward and results in the isolation of gram amounts of the cluster with a variety of counter cations. The transition metal derivatives are, like the ligand, stable towards moisture and air. Complexes with a variety of transition metals (Fe, Ni, Mo, Rh, Ir, Pt) have been synthesized in excellent yield.^[9, 10, 23] Herein, we present syntheses and reactions of platinum and palladium complexes of stanna-*closo*-dodecaborate and the first results of studies on the properties of the [SnB₁₁H₁₁] ligand.

[a] Prof. Dr. L. Wesemann, T. Marx, Dr. I. Pantenburg
Institut für Anorganische Chemie
Universität zu Köln
Greinstrasse 6, 50939 Köln (Germany)
Fax: (+49) 221-470-5083
E-mail: lars.wesemann@uni-koeln.de

[b] Dr. S. Dehnen
Institut für Anorganische Chemie
Universität Karlsruhe
Engesserstrasse, Geb. 30.45
76128 Karlsruhe (Germany)
E-mail: dehnen@achibm6.chemie.uni-karlsruhe.de

Results and Discussion

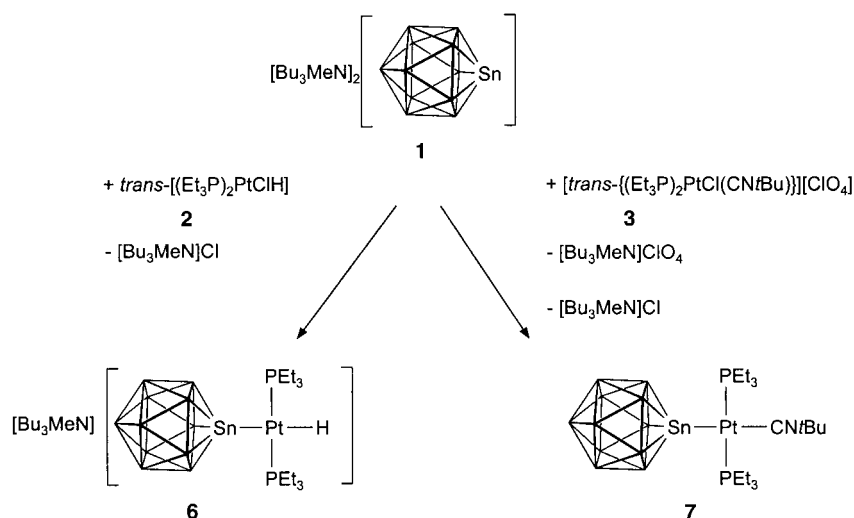
Preparation of stanna-closo-dodecaborate complexes of platinum:

The *trans* influence and the *trans* effect are very important concepts in the chemistry of tetracoordinate d⁸-transition metal complexes. The kinetic *trans* effect of a ligand, L, describes the effect of L on the rate of substitution of the ligand in the *trans* position to L.^[11] The thermodynamic *trans* influence is defined as the weakening of the bond *trans* to L in the equilibrium state.^[12] Therefore, the *trans* influence of a ligand can be determined from spectroscopic data or from results of X-ray crystal structure analyses of the respective square-planar transition metal complexes. To determine the *trans* influence of the stanna-closo-dodecaborate ligand **1**, complexes were synthesized with a variety of ligands *trans* to the heteroborate. The tin nucleophile **1** was allowed to react with the platinum–phosphanes *trans*-[(Et₃P)₂Pt(Cl)H] (**2**), *trans*-[(Et₃P)₂PtCl(CN*t*Bu)]⁺ (**3**), *trans*-[(Et₃P)₂PtCl(CO)]⁺ (**4**), and [(Et₃P)₃PtCl]⁺ (**5**). In the cases of **2** and **3**, the chlorine ligand is readily substituted by the tin nucleophile at room temperature, and the products (**6** and **7**) are obtained in high yield (Scheme 1).

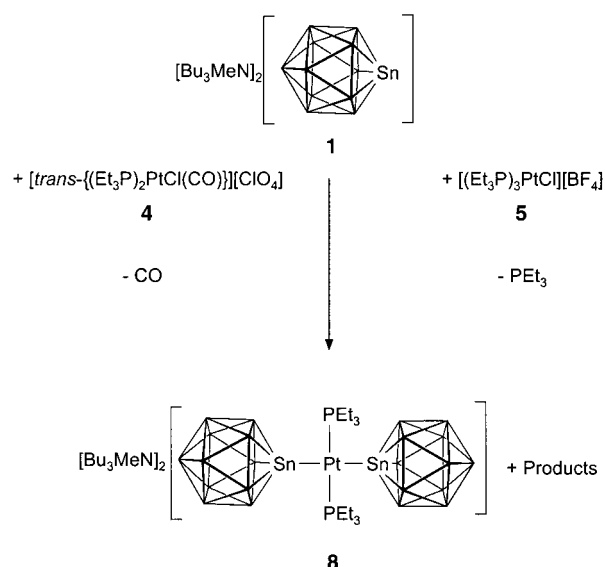
Complexes **4** and **5** react with the nucleophile to form the double substitution product **8** in almost 50% yield, the respective ligand (CO or PEt₃), and undefined platinum compounds (Scheme 2). The synthesis of compound **8** from *cis*-[(Et₃P)₂PtCl₂] and two equivalents of [SnB₁₁H₁₁]²⁻ has been published.^[10]

All the stannaborate complexes presented here are resistant towards moisture and air and are characterized by elemental analysis, IR, and NMR spectroscopy. In the cases of the zwitterion **7**, the five-coordinate complex **9**, [(triphos)Pt(SnB₁₁H₁₁)] (**10**), (triphos = 1,1,1-tris(diphenylphosphanylmethyl)ethane) and the palladium salt **12**, the solid-state structure is determined by X-ray crystal structure analyses.

The progress of the reactions between the nucleophile **1** and the transition metal chlorides (Scheme 1 and Scheme 2) can be monitored by ¹¹B and ³¹P NMR spectroscopy. During the



Scheme 1. Reactions of the stanna-closo-dodecaborate ligand **1** with **2** and **3** to give **6** and **7**, respectively. An unmarked vertex in the cluster corresponds to a BH unit.



Scheme 2. The reaction of **1** with platinum salts **4** and **5** to give **8** in approximately 50% yield. The other platinum-containing products are not yet characterized.

reaction, the signals in the ¹¹B NMR spectrum that arise from the eleven boron atoms shift from $\delta = -5.5$ (B12), -10.9 (B2–B6), and -12.2 (B7–B11) to $\delta = -11$ (B12) and -15 (B2–B11). The coupling between the tin and phosphorus nuclei indicates the formation of a cluster transition metal bond. Satellites with an intensity ratio consistent with the natural ¹¹⁷Sn/¹¹⁹Sn abundance are detected in the ³¹P NMR spectrum of complexes **6** and **9**. ³¹P NMR data for complexes **6–9** are listed in Table 1. The ²J(Sn,Pt,P) coupling constants permit unambiguous assignment of the stereochemistry in the Pt^{II} complexes.^[13] Large coupling constants of around 2000–3000 Hz were observed for complexes with *trans* geometry of the phosphorus and tin substituent. The coupling constants in complex **6** (199 Hz) and **9** (210 Hz) suggest *cis*-Sn–P stereochemistry.

The frequencies of the Pt–H stretch in complex **6** and of the C–N vibration in the zwitterion **7** were measured by IR spectroscopy to investigate the *trans* influence of the stannaborate ligand. A value of 2061 cm⁻¹ was observed for the Pt–H stretch frequency, which indicates that this bond is weakened by the cluster ligand. The value is close to that of a cyanide derivative *trans*-[(Et₃P)₂PtH(CN)] (2041 cm⁻¹) in a series of hydride complexes of type *trans*-[(Et₃P)₂PtH(L)] which has the largest *trans* influence. Therefore, the stannaborate ligand has a larger *trans* weakening influence than, for example, SnCl₃ (2105 cm⁻¹), PEt₃ (2090 cm⁻¹), or CO (2129 cm⁻¹) ligand.^[12] A vibration at 2214 cm⁻¹ is observed for

Table 1. ^{31}P NMR data for the substitution products.

	^{31}P NMR shift [ppm]	$^1J(\text{Pt},\text{P})$ [Hz]	$^2J(^{117}\text{Sn}/^{119}\text{Sn}-\text{Pt}-\text{P})$ [Hz]
6	20.8	2455	199
7	35.6	2117	[a]
8 ^[10]	11.9	2041	214
9	−2.6	1633	240

[a] Due to the low solubility of **7** the satellites were not observed.

the isocyanide CN in complex **7**, which indicates an increase in the CN force constant with respect to that of uncoordinated isocyanide (2134 cm^{-1}).^[14] Since the complexes *trans*- $[(\text{Et}_3\text{P})_2\text{PtH}(\text{CNMe})][\text{ClO}_4]$ (2270 cm^{-1}),^[15] *trans*- $[(\text{Et}_3\text{P})_2\text{PtH}(\text{CNMe})][\text{SO}_3\text{F}]$ (2238 cm^{-1}),^[15] and *trans*- $[(\text{Et}_3\text{P})_2\text{PtCl}(\text{CN}t\text{Bu})][\text{ClO}_4]$ (2211 cm^{-1}),^[14, 16] which have a hydride or chloride ligand *trans* to the isocyanide ligand, exhibit a similar value for the CN force constant, it is difficult to discuss the *trans* influence on the basis of these data.

Single crystals of the polar molecule **7**, which are suitable for X-ray crystal structure analyses, are obtained by slow diffusion of hexane or methanol into a solution of the zwitterion in dichloromethane. The complex crystallizes as yellow cubes in the monoclinic space group $P2_1/n$. Figure 1

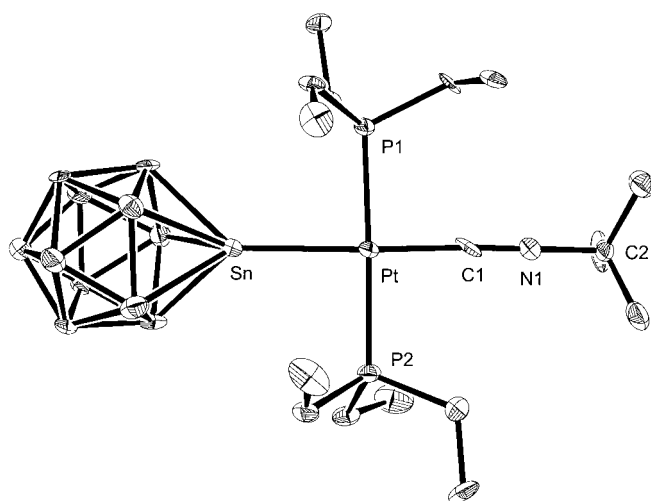


Figure 1. Molecular structure of **7**. Selected bond lengths [Å] and angles [°] (with estimated standard deviations in parentheses): Pt–P1 2.333(2), Pt–P2 2.340(2), Pt–Sn 2.590(1), Pt–C1 1.913(10), C1–N1 1.195(12), N1–C2 1.479(12); N1–C1–Pt 176.5(8), C1–N1–C2 177.9(8), P1–Pt–C1 90.5(3), P2–Pt–C1 92.0(3), P1–Pt–Sn 87.2(1), P2–Pt–Sn 90.9(1), P1–Pt–P2 175.0(1), Sn–Pt–C1 171.7(3).

shows the predicted square-planar coordination of the four ligands around the platinum center. The Pt–P bond length of *trans* coordinated PEt_3 ligands lies within the range of values known from the literature: for example, the *trans*- $[(\text{Et}_3\text{P})_2\text{Pt}(\text{COC}_6\text{H}_5)\text{SnCl}_3]$ has Pt–P bond lengths of 2.324(4) Å and 2.329(4) Å.^[17] The Sn–Pt bond length of 2.590(1) Å can be compared with the Sn–Pt bond lengths in *trans*- $[(\text{Ph}_3\text{P})_2\text{PtPh}(\text{SnB}_{11}\text{H}_{11})]^-$ (2.651(1) Å),^[10] *trans*- $[(\text{Ph}_3\text{P})_2\text{PtH}(\text{SnCl}_3)]$ (2.601(4) Å)^[18] and *trans*- $[(\text{Et}_3\text{P})_2\text{Pt}(\text{COC}_6\text{H}_5)\text{SnCl}_3]$ (2.634(1) Å).^[17] The Pt–C and C–N bond lengths of 1.913(10) Å and 1.195(12) Å, respectively, are typical for isocyanide coordination at Pt^{II} which indicate weak π

donation from the metal to the ligand. (Comparable complexes include: *cis*- $[(\text{MeNC})_2\text{PtMe}_2]$: Pt–C 1.979(8), N–C 1.157(9) Å;^[19] *cis*- $[(\text{PhNC})_2\text{PtCl}_2]$: Pt–C 1.880(18), 1.912(22), N–C 1.19(2), 1.14(3) Å)^[20]

Density functional theory (DFT) calculations of the dipole moment:

The betaine **7** is inert towards moisture and only soluble in polar solvents like dichloromethane. Quantum chemical investigations using the TURBOMOLE program system were carried out to explain these properties.^[21] The calculations were performed with DFT methods,^[22] which in the past have proved to be suitable for the theoretical description of transition metal compounds and have been employed on another Pt– $\text{SnB}_{11}\text{H}_{11}$ complex.^[9] The structural data were used as starting vectors in C_1 symmetry to simultaneously optimize the electronic and geometric structure. The relevant interatomic distances of the calculated model are compared to the experimental results from the X-ray structure analysis in Table 2.

Table 2. Selected interatomic distances [Å] and bond angles [°] for *trans*- $[(\text{Et}_3\text{P})_2\text{Pt}(\text{SnB}_{11}\text{H}_{11})(\text{CN}t\text{Bu})]$ calculated with DFT methods. The numbering of the atoms is identical to those in the experimentally observed compound **7** (Figure 1, experimental values given again in parentheses).

Pt–P1	2.395 (2.333)	N1–C2	1.447 (1.479)	P1–Pt–Sn	85.5 (87.2)
Pt–P2	2.396 (2.340)	N1–C1–Pt	173.3 (1.765)	P2–Pt–Sn	86.4 (90.9)
Pt–Sn	2.689 (2.590)	C1–N1–C2	177.9 (1.779)	P1–Pt–P2	171.6 (175.0)
Pt–C1	1.979 (1.913)	P1–Pt–C1	94.2 (90.5)	Sn–Pt–C1	171.0 (171.7)
C1–N1	1.185 (1.195)	P2–Pt–C1	94.2 (92.0)		

Table 2 shows that the geometric parameters are well reproduced by this quantum chemical treatment. The bond lengths are slightly too long (to a maximum of 0.10 Å for Pt–Sn or 0.06 Å for the Pt–P donor bonds). This is a common fault of DFT methods as dispersion interactions are not considered explicitly. Other interatomic distances differ by up to a maximum of 0.03 Å from the experimental values. Measured and computed angles differ by only 0–4°. The satisfactory reproduction of the X-ray structure of **7** by DFT calculations allows the evaluation of the dipole moment. An elongation of about 0.10 Å in the Pt–Sn bond length has been shown^[9] to influence the dipole moment by less than 10%. A dipole moment of 29.1 D is determined for the optimized structure of *trans*- $[(\text{Et}_3\text{P})_2\text{Pt}(\text{SnB}_{11}\text{H}_{11})(\text{CN}t\text{Bu})]$ by calculation of the expectation value of the dipole operator in the DFT wave function (i.e. the electronic part of the dipole moment) and of the electrostatic moment caused by the nuclei. The result agrees well with the experimental observation that highly polar solvents are required to solvate compound **7**. Comparable dipole moments for zwitterions have been found by AM1 calculations in tetraalkylammonium-arylborate compounds ($\text{Me}_3\text{N}-\text{C}_6\text{H}_4-\text{BnBu}_3$: 20.0 D) and by DFT methods for platinum or rhodium *closo*-borate clusters ($[(\text{bipy}')\text{Pt}(\text{Bz})(\text{Ph})(t\text{Bu}-\text{NC})(\text{SnB}_{11}\text{H}_{11})]$: 28.9 D; $[\text{Cp}^*\text{M}(\text{bipy}')(\text{SnB}_{11}\text{H}_{11})]$: 25.7 D; $\text{bipy}' = 4,4'$ -di-*tert*-butyl-2,2'-bipyridine).^[9, 23]

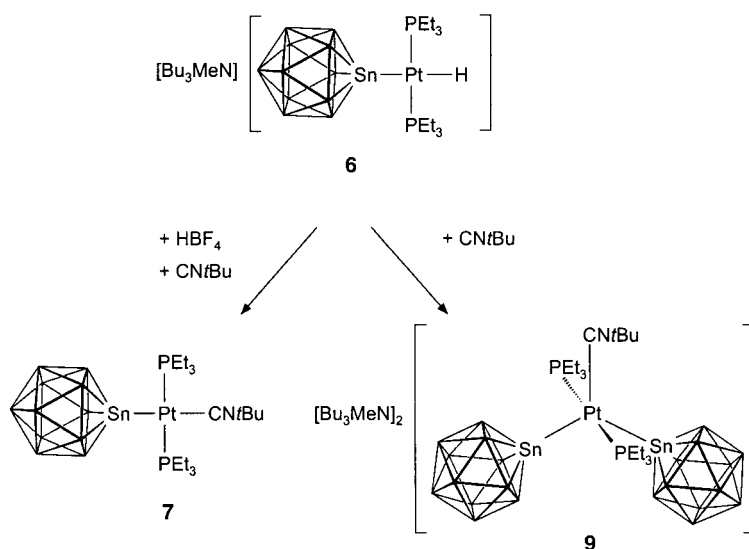
Reactivity of the hydride complex 6: We investigate here the stannaborate dianion ligand and the chemistry of its respec-

tive transition metal complexes. We present here reactions of the hydride complex **6**. The five-coordinate complex **9** is isolated in almost 50% yield from the reaction between the isocyanide (*t*BuNC) and complex **6** (Scheme 3).

The insertion of isocyanide into a Pt–H bond has been observed,^[15] but in this case, there was no evidence that this reaction type occurs. Instead, a stannaborate ligand migrates to another platinum center. The fate of the hydride substituent is unknown, since we have been unable to characterize the other platinum-containing products. In the ¹H NMR spectra of the reaction mixture, only the disappearance of the hydride is detected. Apart from the signal from the five-coordinate complex, a variety of undefined resonances are found in the ³¹P NMR spectrum. The signal in the ³¹P NMR spectrum is very broad due to the high mobility of the platinum complex. The ²J_{Sn,P} and ¹J_{P,Pt} coupling constants were determined from a measurement at –80 °C. A Sn–P coupling constant of 240 Hz and a Pt–P coupling constant of 1633 Hz are obtained. These values suggest a cisoid ordering of the stannaborate to PEt₃ ligands. Two isomers with cisoid configuration of the tin and phosphorus ligands are possible in solution. We suggest that isomer **B** in Figure 2 exists in solution on the basis of the ²J_{Pt,P} coupling constant of 1633 Hz which is smaller than typical *trans* ²J_{Pt,P} coupling constants of around 2500 Hz.^{[10], [13]}

Isomer **A** is found in the solid state. Single crystals of the salt [Bu₃MeN]₂[*trans*-{(Et₃P)₂Pt(SnB₁₁H₁₁)₂(CN*t*Bu)}] (**9**) were obtained by slow diffusion of methanol into a saturated dichloromethane solution. The stannaborate platinum complex crystallizes in the monoclinic space group *C2/c* with disorder of the isocyanide ligand. The coordination sphere around the platinum center (Figure 3) can be described as a trigonal bipyramid with phosphane ligands occupying the axial positions.

Pentacoordination is known for a variety of platinum complexes such as [Pt[P(OCH₃)₃]₅]^[29] or [Pt(SnCl₃)₄PEt₃]^{[2–, [30]} Such species have been investigated with respect to their solution dynamics, stereochemistry, and mechanistic importance. [Pt(SnCl₃)₅]^{3–} is of particular interest since it catalyzes the homogeneous hydrogenation of ethylene and acetylene



Scheme 3. The synthesis of **7** and **9** from **6**.

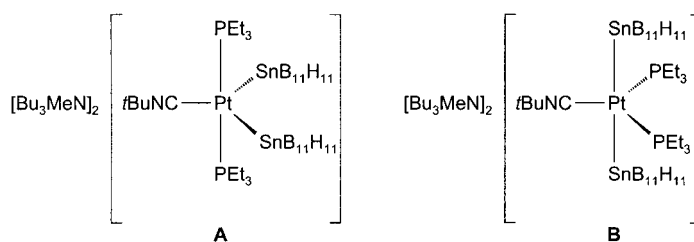


Figure 2. Isomers of the dianion of **9** with cisoid orientation between the phosphane and stannaborate ligands.

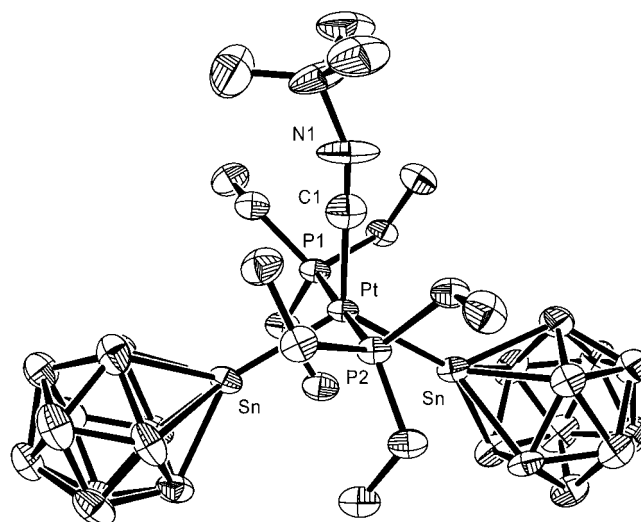
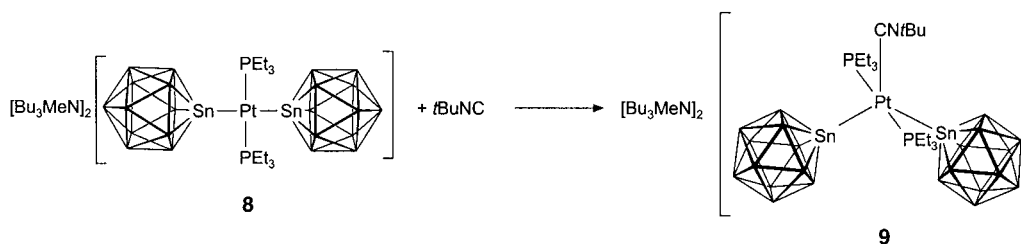


Figure 3. Molecular structure of **9**. Selected bond lengths [Å] and angles [°] (with estimated standard deviations in parentheses): Pt–P 2.337(2), Pt–Sn 2.640(1), Pt–C1 1.995(15), C1–N1 1.18(2), N1–C8 1.550(10); C1–Pt–P 89.07(5), P–Pt–Sn 92.34(5), C1–Pt–Sn 120.3(1), N1–C1–Pt 180.0(2), C1–N1–C8 156.5(2).

under mild conditions.^[5, 31] The Pt–P bond length of the axially coordinated phosphane ligand is 2.337(2) Å, which is similar to Pt–P distance in the ylide **7** or in [(Et₃P)₂Pt(C(O)C₆H₅)SnCl₃] (2.324(4), 2.329(4) Å).^[17] The clusters coordinate at the platinum center with a Pt–Sn bond length of 2.640(1) Å which is in the range of other Pt–SnB₁₁H₁₁ complexes^[10] and which is close to Pt–Sn bond length in [Pt(SnCl₃)₅]^{3–} (2.551(1)–2.572(1) Å).^[31] The isocyanide coordinates to the transition metal and exhibits Pt–C and C–N bond lengths of 1.995(12) and 1.18(2) Å, respectively. These values are similar to those in **7** and reflect weak π donation from the Pt^{II} metal to the ligand. The C–N stretching frequency of 2190 cm^{–1} is close to that of uncoordinated isocyanide (2214 cm^{–1}).^[14] The pentacoordinate complex can also be synthesized from the reaction of the tetracoordinate dianion **8** with isocyanide. This is, however, the only example of

Scheme 4. Reaction of **8** with *t*BuNC to give **9**.

the formation of such an adduct. Other Lewis bases such as CO, alkenes, pyridine, Et₃N, and Ph₃P do not react. (Scheme 4)

According to the procedure outlined in Scheme 3, we attempted the synthesis of other stannaborate zwitterions like **7** by reacting the hydride **6** with HBF₄ and the respective donor ligand. We did not isolate any of the respective zwitterionic molecules from reaction with THF, PPh₃, CO, 4-*t*Bu-pyridine or cyclohexene. So far only isocyanide stabilizes such an adduct. Interestingly, we were not able to synthesize a square-planar coordinated platinum(II) complex (Scheme 2 and 3) with a monodentate phosphine ligand *trans* to the stannaborate although we have already synthesized the [(triphos)Pt(SnB₁₁H₁₁)] (**10**) zwitterion.^[10] In view of these results we were interested in the Pt–P distances in the complex [(triphos)Pt(SnB₁₁H₁₁)] (**10**) which was synthesized from [(triphos)PtCl]BF₄ and **1** in high yield. Crystals suitable for X-ray crystal structure analyses were obtained by slow diffusion of methanol into a solution of **10** in dimethyl sulfoxide. The zwitterion crystallizes in the triclinic space group *P* $\bar{1}$. Figure 4 shows the molecular

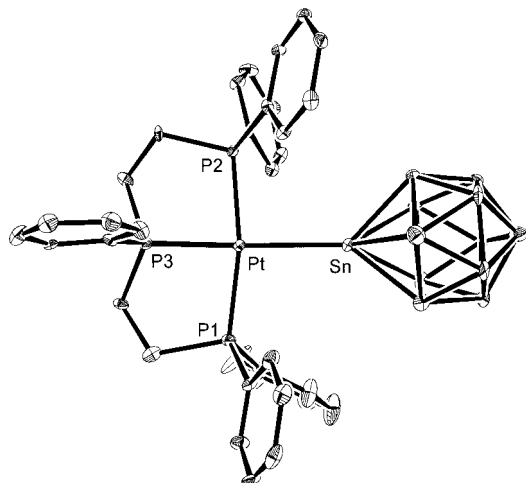


Figure 4. Molecular structure of **10**. Selected bond lengths [\AA] and angles [$^\circ$] (with estimated standard deviations in parentheses): Pt–P1 2.305(3), Pt–P2 2.315(3), Pt–P3 2.270(3), Pt–Sn 2.626(1); P3–Pt–P1 84.68(11), P3–Pt–P2 84.77(11), P1–Pt–Sn 97.1(1), P2–Pt–Sn 93.7(1), P1–Pt–P2 167.35(11), P3–Pt–Sn 177.7(1).

structure of **10** in which the platinum center is nearly square planar: Pt–P bond lengths are 2.305(3), 2.315(3), and 2.270(3) \AA (*trans* to Sn). Comparison of these Pt–P bond lengths with those from [(triphos)PtCl]Cl (2.312(2), 2.315(2), and 2.207(2) \AA ; *trans* to Cl) shows that there is a slight

increase of the Pt–P separation, for that positioned *trans* to the tin ligand. This small effect may be attributed to the stronger *trans* influence of the stannaborate substituent with respect to that of the chlorine ligand. The Pt–Sn bond length of 2.626(1) \AA lies within the range of those in the platinum complexes **7** and **9**.

Orientation of the dipoles **7 and **10** in the solid state:** The dipole packing may be discussed with reference to the results of the crystal structure analyses of the zwitterionic molecules **7** (Figure 5) and **10** (Figure 6). The strong dipole moments of both zwitterions are aligned along the Sn–Pt bond, which is

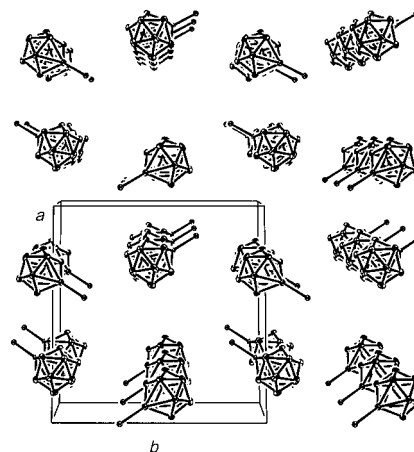


Figure 5. Schematic view of the arrangement of **7** in the crystal along the *c* axis;^[42] the Pt–SnB₁₁ fragment is shown, other atoms are omitted for clarity.

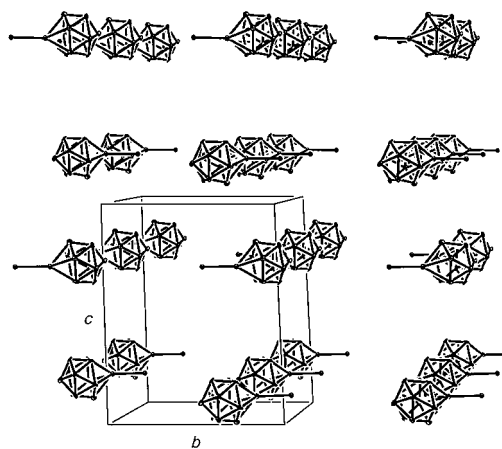
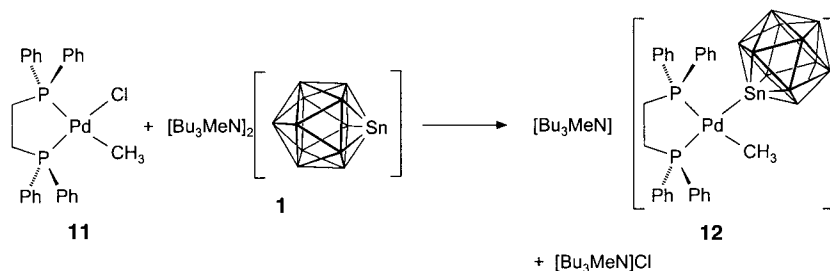


Figure 6. Schematic view of the arrangement of **10** in the crystal along the *a* axis;^[42] the Pt–SnB₁₁ fragment is shown, other atoms are omitted for clarity.

directed from the transition metal complex towards the cluster unit. The polar molecules are packed in layers with a resulting dipole moment. These layers stack such that stacks of molecules with alternating dipole moment orientations result.

Synthesis of a palladium complex: The synthesis of a variety of platinum-stannaborate complexes led us to investigate this chemistry in palladium. Nucleophilic substitution between stannaborate **1** and palladium chloride **11** forms the first palladium complex of the stanna-*closo*-dodecaborate ligand in 88% yield (Scheme 5).



Scheme 5. Reaction of **11** and **1** to give **12**, the first stanna-*closo*-dodecaborate complex of palladium.

This salt is, like the platinum complexes, resistant towards moisture and air and is characterized by elemental analysis and NMR spectroscopy. A signal at $\delta = -14.1$ in the ^{11}B NMR spectrum (for ten boron atoms; the signal for B12 was not observed) typically indicates successful substitution of the heteroborate. As expected, two resonances were observed in the ^{31}P NMR spectrum at $\delta = 49.7$ (*cis* to Sn: $^2J_{\text{P,Sn}} = 298$ Hz) and $\delta = 56.9$ (*trans* to Sn: $^2J_{\text{P,Sn}} = 2542$ Hz). The spectrum is interpreted on the basis that the *trans* P-Pd-Sn coupling constant is larger than that of the *cis* complex.^[13] An X-ray crystal structure analysis on a single crystal of **12** was carried out to establish the structure of the salt in the solid state. Compound **12** crystallizes as yellow rods in the space group $P2_1/c$. The molecular structure of the anion of **12** is shown in Figure 7.

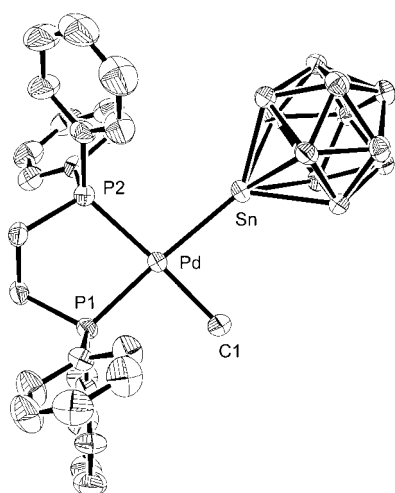


Figure 7. Molecular structure of **12**. Selected bond lengths [Å] and angles [°] (with estimated standard deviations in parentheses): Pd–Cl 2.123(6), Pd–P1 2.279(2), Pd–P2 2.312(2), Pd–Sn 2.567(1); C1–Pd–P1 91.7(1), P1–Pd–P2 85.4(1), C1–Pd–Sn 85.7(1), P2–Pd–Sn 97.9(1), P1–Pd–Sn 173.6(1), P2–Pd–Cl 173.4(2).

The substituents around the palladium atom describe a square planar configuration; the Pd–Sn bond length of 2.567(1) Å is close to that in $(\text{Me}_2\text{SnCH}_2\text{CH}_2\text{PPh}_2)\text{-Pd}(\text{Ph}_2\text{PCH}_2\text{CH}_2\text{SiMe}_2)$ (2.573(1) Å).^[32] The Pd–P bond length of 2.312(2) Å *trans* to the methyl group is longer than that *trans* to the stannaborate substituent (2.279(2) Å). The comparison of the Pd–P bond lengths in $[(\text{dppe})\text{Pd}(\text{CH}_2\text{Cl})\text{Cl}]$ (dppe = 1,2-bis(diphenylphosphany)ethane; Pd–P *trans* to CH_2Cl 2.309(1) Å; *trans* to Cl 2.232(1) Å)^[33] and in **12** leads to the conclusion that the stannaborate ligand exhibits a *trans* influence stronger than chloride and weaker than methyl.

Conclusion

The results presented herein show that, in transition metal chemistry, the stanna-*closo*-dodecaborate cluster is a ligand with a stronger *trans* influence than SnCl_3 , CO, PR_3 , Cl, or alkene ligands. Furthermore, the ligand is labile with respect

to substitution reactions in square planar coordinated platinum complexes. This leads in some cases to the transfer of the tin ligand to another transition metal center and the formation of di(stannaborate) complexes.

Experimental Section

All manipulations were carried out under dry N_2 in Schlenk glassware; solvents were dried and purified by standard methods and stored under N_2 ; NMR Bruker AC 200 (^1H : 200 MHz, internal TMS; $^{13}\text{C}\{^1\text{H}\}$: 50 MHz, internal TMS; $^{31}\text{P}\{^1\text{H}\}$: 81 MHz, external 85% H_3PO_4 ; $^{11}\text{B}\{^1\text{H}\}$: 64 MHz, external $\text{BF}_3 \cdot \text{Et}_2\text{O}$); elemental analysis: Institut für Anorganische Chemie der Universität zu Köln, Heraeus C,H,N,O-Rapid elemental analyser; IR spectrometer: IFS66v/s Bruker; *trans*- $[(\text{PEt}_3)_2\text{Pt}(\text{H})\text{Cl}]$,^[34] *trans*- $[(\text{PEt}_3)_2\text{Pt}(\text{tBu-NC})\text{Cl}][\text{ClO}_4]$,^[16] $[\text{Bu}_3\text{MeN}]_2[\text{trans}\{-\{(\text{PEt}_3)_2\text{Pt}(\text{SnB}_{11}\text{H}_{11})_2\}]$,^[10] and $[(\text{dppe})\text{Pd}(\text{Me})\text{Cl}]$ ^[35] were prepared by published methods.

$[\text{Bu}_3\text{MeN}][\text{trans}\{-\{(\text{PEt}_3)_2\text{Pt}(\text{H})(\text{SnB}_{11}\text{H}_{11})\}]$ (6**):** $[\text{Bu}_3\text{MeN}]_2[\text{SnB}_{11}\text{H}_{11}]$ (0.71 g, 1.09 mmol) in CH_2Cl_2 (20 mL) was added to a solution of *trans*- $[(\text{PEt}_3)_2\text{Pt}(\text{H})\text{Cl}]$ (0.51 g, 1.09 mmol) in CH_2Cl_2 (20 mL) and stirred for 12 h. The solvent was evaporated in vacuo and the residue was washed with water to remove $[\text{Bu}_3\text{MeN}]\text{Cl}$. The product was isolated by filtration, dried in vacuo, and recrystallized from CH_2Cl_2 by slow diffusion of hexane at 8 °C to give **6** (0.41 g, 85% yield) as orange crystals; ^1H NMR (200 MHz, CD_2Cl_2 , 25 °C): $\delta = -7.15$ (t, $^1J_{\text{H,Pt}} = 1312$ Hz, $^2J_{\text{H,P}} = 11.6$ Hz, 1H; PtH), 1.01 (t, $^3J = 7.2$ Hz, 9H; CH_2CH_3), 1.13 (m, 18H; PCH_2CH_3), 1.44 (m, 6H; $\text{CH}_2\text{CH}_2\text{CH}_3$), 1.65 (m, 6H; $\text{CH}_2\text{CH}_2\text{CH}_2$), 2.14 (m, 12H; PCH_2CH_3), 3.07 (s, 3H; NCH_3), 3.23 (m, 6H; NCH_2CH_2); $^{11}\text{B}\{^1\text{H}\}$ NMR (64 MHz, CD_2Cl_2 , 25 °C): $\delta = -9.2$ (s; B12), -14.5 (s; B2/B3/B4/B5/B6, B7/B8/B9/B10/B11); $^{13}\text{C}\{^1\text{H}\}$ NMR (50 MHz, CD_2Cl_2 , 25 °C): $\delta = 9.4$ (s; PCH_2CH_3), 13.8 (s; CH_2CH_3), 20.0 (s; $\text{CH}_2\text{CH}_2\text{CH}_3$), 22.1 (m, br; PCH_2CH_3), 24.7 (s; $\text{CH}_2\text{CH}_2\text{CH}_2$), 49.5 (s; NCH_3), 62.3 (s; NCH_2CH_2); $^{31}\text{P}\{^1\text{H}\}$ NMR (81 MHz, CD_2Cl_2 , 25 °C): $\delta = 20.8$ (s, $^1J_{\text{Pt,P}} = 2455$ Hz, $^2J_{\text{P,Sn}} = 199$ Hz; in *cis* position to $\text{SnB}_{11}\text{H}_{11}$); IR (KBr): $\tilde{\nu} = 2061$ cm^{-1} (Pt–H); elemental analysis calcd (%) for $\text{C}_{25}\text{H}_{22}\text{B}_{11}\text{NP}_2\text{PtSn}$ (881.50): C 34.06, H 8.23, N 1.59; found: C 33.95, H 8.10, N 2.09.

***trans*- $[(\text{PEt}_3)_2\text{Pt}(\text{tBuNC})(\text{SnB}_{11}\text{H}_{11})]$ (**7**):** Method a: *trans*- $[(\text{PEt}_3)_2\text{Pt}(\text{tBuNC})(\text{Cl})][\text{ClO}_4]$ (0.36 g, 0.55 mmol) in CH_2Cl_2 (20 mL) was treated with a solution of $[\text{Bu}_3\text{MeN}]_2[\text{SnB}_{11}\text{H}_{11}]$ (0.36 g, 0.55 mmol) in CH_2Cl_2 (20 mL). The reaction was stirred at room temperature for 12 h. The solvent was evaporated in vacuo and the residue was washed with water to

remove Bu_3MeN salts. The product was isolated by filtration, dried in vacuo and recrystallized from CH_2Cl_2 by slow diffusion of hexane to give **2** (0.38 g, 92% yield) as bright yellow cubes. Method b: $\text{trans}[(\text{PEt}_3)_2\text{Pt}(\text{H})(\text{SnB}_{11}\text{H}_{11})][\text{Bu}_3\text{MeN}]$ (0.20 g, 0.23 mmol) in a mixture of CH_2Cl_2 (10 mL) and THF (10 mL) was stirred at 0°C with HBF_4 (0.031 mL, 54% in Et_2O , $\rho = 1.19\text{ g mL}^{-1}$, 0.23 mmol) for 5 min before the addition of $t\text{BuNC}$ (0.2 mL). The reaction mixture was stirred at room temperature for 2 h and the product crystallized by slow diffusion of methanol into the reaction mixture at 8°C to give **7** (0.15 g, 82% yield) as yellow cubes; $^1\text{H NMR}$ (200 MHz, $[\text{D}_6]\text{DMSO}$, 25°C): $\delta = 1.13$ (m, 18H; PCH_2CH_3), 1.17 (s, 9H; $\text{C}(\text{CH}_3)_3$), 2.40 (m, 12H; PCH_2CH_3); $^{11}\text{B}\{^1\text{H}\}$ NMR (64 MHz, $[\text{D}_6]\text{DMSO}$, 25°C): $\delta = -14.1$ (s; B2/B3/B4/B5/B6, B7/B8/B9/B10/B11); $^{13}\text{C}\{^1\text{H}\}$ NMR (50 MHz, $[\text{D}_6]\text{DMSO}$, 25°C): $\delta = 9.3$ (s; PCH_2CH_3), 21.5 (m, br; PCH_2CH_3), 28.8 (s; $\text{C}(\text{CH}_3)_3$), 34.5 (s; $\text{C}(\text{CH}_3)_3$); $^{31}\text{P}\{^1\text{H}\}$ NMR (81 MHz, $[\text{D}_6]\text{DMSO}$, 25°C): $\delta = 35.6$ (s; $^1J_{\text{Pt,P}} = 2117\text{ Hz}$; Et_3Ppt); IR (KBr): $\tilde{\nu} = 2214\text{ cm}^{-1}$ (NC); elemental analysis calcd (%) for $\text{C}_{17}\text{H}_{30}\text{B}_{11}\text{NP}_2\text{PtSn}$ (763.24): C 26.78, H 6.68, N 1.84; found: C 27.38, H 6.65, N 2.10.

$[\text{Bu}_3\text{MeN}]_2[(\text{PEt}_3)_2\text{Pt}(\text{SnB}_{11}\text{H}_{11})_2(t\text{BuNC})]$ (9**):** Method a: At room temperature, $t\text{BuNC}$ (0.2 mL) was added to $[(\text{PEt}_3)_2\text{Pt}(\text{H})(\text{SnB}_{11}\text{H}_{11})][\text{Bu}_3\text{MeN}]$ (0.20 g, 0.23 g) in CH_2Cl_2 (20 mL). After 30 min, slow diffusion of methanol into the reaction mixture at 8°C yielded **9** (0.12 g, 37% yield) as yellow needles. Method b: At room temperature, $t\text{BuNC}$ (0.2 mL) was added to $[\text{Bu}_3\text{MeN}]_2[\text{trans}\{(\text{PEt}_3)_2\text{Pt}(\text{SnB}_{11}\text{H}_{11})_2\}]$ (0.43 g, 0.32 mmol) in CH_2Cl_2 (20 mL) and stirred for 30 min. Complex **9** (0.45 g, 88% yield) was isolated by crystallization according to the procedure outlined in Method a; $^1\text{H NMR}$ (200 MHz, $[\text{D}_6]\text{DMSO}$, 25°C): $\delta = 0.92$ (t, $^3J = 7.2\text{ Hz}$, 18H; CH_2CH_3), 1.14 (m, 18H; PCH_2CH_3), 1.25 (m, 12H; $\text{CH}_2\text{CH}_2\text{CH}_3$), 1.52 (s, 9H; $\text{C}(\text{CH}_3)_3$), 1.58 (m, 12H; $\text{CH}_2\text{CH}_2\text{CH}_2$), 2.34 (m, 12H; PCH_2CH_3), 2.93 (s, 6H; NCH_3), 3.18 (m, 12H; NCH_2CH_2); $^{11}\text{B}\{^1\text{H}\}$ NMR (64 MHz, $[\text{D}_6]\text{DMSO}$, 25°C): $\delta = -14.1$ (s; B2/B3/B4/B5/B6, B7/B8/B9/B10/B11); $^{13}\text{C}\{^1\text{H}\}$ NMR (50 MHz, $[\text{D}_6]\text{DMSO}$, 25°C): $\delta = 9.5$ (s; PCH_2CH_3), 13.5 (s; CH_2CH_3), 19.2 (s; $\text{CH}_2\text{CH}_2\text{CH}_3$), 22.1 (m, br; PCH_2CH_3), 23.4 (s; $\text{CH}_2\text{CH}_2\text{CH}_2$), 29.1 (s; $\text{C}(\text{CH}_3)_3$), 47.5 (s; NCH_3), 59.1 (s; $\text{C}(\text{CH}_3)_3$), 60.4 (s; NCH_2CH_2), 178.1 (s; $t\text{BuNC}$); $^{31}\text{P}\{^1\text{H}\}$ NMR (81 MHz, $[\text{D}_6]\text{DMSO}$, -80°C): $\delta = -2.6$ (s, $^1J_{\text{Pt,P}} = 1633\text{ Hz}$, $^1J_{\text{Pt,Sn}} = 240\text{ Hz}$; in *cis* position to $\text{SnB}_{11}\text{H}_{11}$); IR (KBr): $\tilde{\nu} = 2190\text{ cm}^{-1}$ (NC); elemental analysis calcd (%) for $\text{C}_{33}\text{H}_{41}\text{B}_{22}\text{N}_3\text{P}_2\text{PtSn}_2$ (1412.71): C 36.56, H 8.63, N 2.97; found: C 36.14, H 8.60, N 3.05.

$[\text{Bu}_3\text{MeN}][(\text{dppe})\text{Pd}(\text{Me})(\text{SnB}_{11}\text{H}_{11})]$ (12**):** A solution of $[(\text{dppe})\text{Pd}(\text{Me})\text{Cl}]$ (1.60 g, 2.88 mmol) in CH_2Cl_2 (60 mL) was added to $[\text{Bu}_3\text{MeN}]_2[\text{SnB}_{11}\text{H}_{11}]$ (1.87 g, 2.88 mmol) in CH_2Cl_2 (20 mL). After 24 h, volatiles were removed in vacuo and the bright yellow residue was washed with water to remove $[\text{Bu}_3\text{MeN}]\text{Cl}$. Crystallization was carried out by slow diffusion of hexane into a saturated solution of **12** in dichloromethane at 8°C to give bright yellow crystals (2.45 g, 88% yield); $^1\text{H NMR}$ (200 MHz, $[\text{D}_6]\text{DMSO}$, 25°C): $\delta = 0.63$ (d/d, $^3J_{\text{H,P}} = 6.4/6.2\text{ Hz}$, 3H; PdCH_3), 0.91 (t, $^3J = 7.1\text{ Hz}$, 9H; CH_2CH_3), 1.28 (m, 6H; $\text{CH}_2\text{CH}_2\text{CH}_3$), 1.59 (m, 6H; $\text{CH}_2\text{CH}_2\text{CH}_2$), 2.60–2.80 (m, 4H; $\text{PCH}_2\text{CH}_2\text{P}$), 3.03 (s, 3H; NCH_3), 3.18 (m, 6H; NCH_2CH_2), 7.30–7.90 (m, 20H; PC_6H_5); $^{11}\text{B}\{^1\text{H}\}$ NMR (64 MHz, $[\text{D}_6]\text{DMSO}$, 25°C): $\delta = -14.1$ (s; B2/B3/B4/B5/B6, B7/B8/B9/B10/B11); $^{13}\text{C}\{^1\text{H}\}$ NMR (50 MHz, $[\text{D}_6]\text{DMSO}$, 25°C): $\delta = -6.3$ (d, $^2J_{\text{C,P}} = 89.2\text{ Hz}$; PdCH_3), 13.5 (s; CH_2CH_3), 19.2 (s; $\text{CH}_2\text{CH}_2\text{CH}_3$), 23.4 (s; $\text{CH}_2\text{CH}_2\text{CH}_2$), 26.6–28.5 (m, br; $\text{PCH}_2\text{CH}_2\text{P}$), 47.6 (s; NCH_3), 60.4 (s; NCH_2CH_2), 128.0–130.0 (m, br; $\text{CH}(\text{PC}_6\text{H}_5)$), 130.5–132.5 (m, br; $\text{CH}(\text{PC}_6\text{H}_5)$), 132.5–134.5 (m, br; $\text{CH}(\text{P}-\text{C}_6\text{H}_5)$); $^{31}\text{P}\{^1\text{H}\}$ NMR (81 MHz, $[\text{D}_6]\text{DMSO}$, 25°C): $\delta = 49.7$ (d, $^2J_{\text{P,P}} = 24\text{ Hz}$, $^2J_{\text{P,Sn}} = 298\text{ Hz}$; Ph_2PCH_2 in *cis* position to $\text{SnB}_{11}\text{H}_{11}$), 56.9 (d, $^2J_{\text{P,P}} = 24\text{ Hz}$, $^2J_{\text{P,Sn}} = 2542\text{ Hz}$; Ph_2PCH_2 in *trans* position to $\text{SnB}_{11}\text{H}_{11}$); elemental analysis calcd (%) for $\text{C}_{40}\text{H}_{68}\text{B}_{11}\text{NP}_2\text{PdSn}$ (968.89): C 49.58, H 7.07, N 1.45; found: C 48.30, H 7.12, N 1.52.

X-ray crystallographic studies: **7:** $\text{C}_{17}\text{H}_{30}\text{B}_{11}\text{NP}_2\text{PtSn}$; formula mass 763.21 g mol^{-1} ; monoclinic space group $P2_1/n$; $a = 10.698(2)$, $b = 17.170(2)$, $c = 17.877(3)\text{ \AA}$, $\beta = 107.26(2)^\circ$, $V = 3136.0(8)\text{ \AA}^3$, $Z = 4$, $\rho_{\text{calcd}} = 1.616\text{ g cm}^{-3}$, $\mu(\text{MoK}\alpha) = 5.363\text{ mm}^{-1}$. Image plate diffractometer (IPDS, Stoe); $\text{MoK}\alpha$ radiation (graphite monochromator, $\lambda = 71.07\text{ pm}$); data collection at 200 K on a single crystal of dimensions $0.2 \times 0.2 \times 0.2\text{ mm}$, $1.7 \leq \theta \leq 24.2^\circ$; 4829 independent reflections measured, 3045 “observed” [$I > 2\sigma(I)$]; data corrections: Lorentz and polarization factors, numerical absorption with programs X-RED and X-Shape (Stoe Darmstadt, 1994);^[36] structure solution by direct methods and difference Fourier synthesis, F^2 refinement;^[37, 38] anisotropic parameters for non-hydrogen atoms. All

hydrogen atoms were placed in calculated positions and refined with isotropic thermal parameters. Convergence was obtained for 298 variables with $wR_2 = 0.0785$, $R_1 = 0.0416$, $\text{Goof} = 0.835$; max. residual density $+0.86$ (1.70 \AA from Pt) e \AA^{-3} . **9:** $\text{C}_{43}\text{H}_{112}\text{B}_{22}\text{N}_3\text{P}_2\text{PtSn}_2$; formula mass 1403.59 g mol^{-1} ; monoclinic space group $C2/c$; $a = 30.573(4)$, $b = 11.5996(14)$, $c = 19.184(3)\text{ \AA}$, $\beta = 94.511(15)^\circ$, $V = 6782.1(15)\text{ \AA}^3$, $Z = 4$, $\rho_{\text{calcd}} = 1.375\text{ g cm}^{-3}$, $\mu(\text{MoK}\alpha) = 2.867\text{ mm}^{-1}$. Image plate diffractometer (IPDS, Stoe); $\text{MoK}\alpha$ radiation (graphite monochromator, $\lambda = 71.07\text{ pm}$); data collection at 170 K on a single crystal of dimensions $0.1 \times 0.2 \times 0.1\text{ mm}$, $1.9 \leq \theta \leq 24.2^\circ$; 5368 independent reflections measured, 3929 “observed” [$I > 2\sigma(I)$]; data corrections: Lorentz and polarization factors; numerical absorption with programs X-RED and X-Shape (Stoe Darmstadt, 1994);^[36] structure solution by direct methods and difference Fourier synthesis, F^2 refinement;^[39, 40, 41] anisotropic parameters for non-hydrogen atoms. Atoms Pt, C7 and N1 lie in special positions on the twofold axis. With the exception of the hydrogen atoms that are connected to the disordered isocyanide ligand, all hydrogen atoms were placed in calculated positions and refined with isotropic thermal parameters. The isocyanide ligand shows a disorder with respect to the twofold axis. Refinement of the non-disordered model in spacegroup $C2$ does not convert. Convergence in $C2/c$ was obtained for 325 variables with $wR_2 = 0.1225$, $R_1 = 0.0456$, $\text{Goof} = 0.804$; max. residual density 1.57 (1.32 \AA from H23C) e \AA^{-3} . **12:** $\text{C}_{40}\text{H}_{68}\text{B}_{11}\text{NP}_2\text{PdSn}$; formula mass 968.89 g mol^{-1} ; monoclinic space group $P2_1/c$; $a = 12.3455(2)$, $b = 18.3136(5)$, $c = 23.1877(7)\text{ \AA}$, $\beta = 101.4121(14)^\circ$, $V = 5138.9(2)\text{ \AA}^3$, $Z = 4$, $\rho_{\text{calcd}} = 1.252\text{ g cm}^{-3}$, $\mu(\text{MoK}\alpha) = 0.925\text{ mm}^{-1}$. Image plate diffractometer (IPDS, Stoe); $\text{MoK}\alpha$ radiation (graphite monochromator, $\lambda = 71.07\text{ pm}$); data collection at 293 K on a single crystal of dimensions $0.1 \times 0.3 \times 0.1\text{ mm}$, $1.4 \leq \theta \leq 27.6^\circ$; 11608 independent reflections measured, 5101 “observed” [$I > 2\sigma(I)$]; data corrections: Lorentz and polarization factors; numerical absorption with programs X-RED and X-Shape (Stoe Darmstadt, 1994);^[36] structure solution by direct methods and difference Fourier synthesis, F^2 refinement;^[39, 40, 41] anisotropic parameters for non-hydrogen atoms. All hydrogen atoms were placed in calculated positions and refined with isotropic thermal parameters. Convergence was obtained for 506 variables with $wR_2 = 0.1423$, $R_1 = 0.0511$, $\text{Goof} = 0.864$; max. residual density 0.99 (2.79 \AA from H9) e \AA^{-3} . **10 · 2 (CH₃)₂SO:** $\text{C}_{38}\text{H}_{44}\text{B}_{11}\text{O}_2\text{P}_3\text{PtS}_2\text{Sn}$; formula mass 1122.45 g mol^{-1} ; triclinic space group $P\bar{1}$; $a = 10.742(2)$, $b = 13.739(2)$, $c = 17.623(3)\text{ \AA}$, $\alpha = 91.70(2)$, $\beta = 106.98(2)$, $\gamma = 107.71(2)^\circ$, $V = 2349.5(6)\text{ \AA}^3$, $Z = 2$, $\rho_{\text{calcd}} = 1.587\text{ g cm}^{-3}$, $\mu(\text{MoK}\alpha) = 3.729\text{ mm}^{-1}$. Image plate diffractometer (IPDS, Stoe); $\text{MoK}\alpha$ radiation (graphite monochromator, $\lambda = 71.07\text{ pm}$); data collection at 170 K on a single crystal of dimensions $0.1 \times 0.3 \times 0.1\text{ mm}$, $2.5 \leq \theta \leq 28.2^\circ$; 10439 independent reflections measured, 4231 “observed” [$I > 2\sigma(I)$]; data corrections: Lorentz and polarization factors; structure solution by direct methods and difference Fourier synthesis, F^2 refinement;^[39, 40, 41] anisotropic parameters for non-hydrogen atoms. With exception of the hydrogen atoms that are connected to the solvent molecules, all hydrogen atoms were placed in calculated positions and refined with isotropic thermal parameters. DMSO molecules are disordered and no hydrogens were calculated. Convergence was obtained for 541 variables with $wR_2 = 0.1157$, $R_1 = 0.052$, $\text{Goof} = 0.663$; max. residual density 1.27 (0.56 \AA from Pt) e \AA^{-3} .

Theoretical methods: The program system TURBOMOLE^[21] was employed to carry out the DFT^[22] investigations using the RIDFT program^[24] with the Becke–Perdew (B-P) functional^[25] and a gridsize of m3. The RIDFT program has been developed from the DFT program^[26] and approximates the coulomb part of the two-electron interactions. Basis sets were of SV(P) quality (SV(P) = split valence plus polarization for all non-hydrogen atoms, split valence for hydrogen atoms).^[27] The Sn and the Pt atom were treated with effective core potentials (ECP) that serve as approximations for inner electrons considering relativistic effects. For Sn, an ECP-46 which described 46 core electrons was used; for Pt, an ECP-60 which described 60 core electrons.^[28] The dipole moment of $\text{trans}\{(\text{Et}_3\text{P})_2\text{Pt}(\text{SnB}_{11}\text{H}_{11})\text{-(CN}t\text{Bu)}\}$ was calculated with the program MOLOCH which was implemented within TURBOMOLE.

Acknowledgements

We thank the Deutsche Forschungsgemeinschaft (Schwerpunktprogramm Polyeder) and the Fonds der Chemischen Industrie for financial support. Moreover, we thank Degussa AG for gifts of chemicals.

- [1] M. S. Holt, W. L. Wilson, J. H. Nelson, *Chem. Rev.* **1989**, *89*, 11–49; J. D. Donaldson, *Prog. Inorg. Chem.* **1968**, *8*, 287–356; E. H. Brooks, R. J. Cross, *Organomet. Chem. Rev.* **1970**, *6A*, 227–282; N. S. Vyazankin, G. A. Razuvaev, O. A. Krugkaya, *Organomet. Chem. Rev.* **1968**, *3A*, 323–423.
- [2] F. Glocking in *Chemistry of Tin*, (Eds.: P. G. Harrison), Chapman and Hall, New York, **1989**, pp. 245–293.
- [3] F. Bonati, G. Wilkinson, *J. Chem. Soc.* **1964**, *A*, 179–181; A. R. Manning, *Chem. Commun.* **1966**, 906; P. Mazerolles, J. Dubac, M. Lesbre, *J. Organomet. Chem.* **1968**, *12*, 143–148.
- [4] J. H. Nelson, N. W. Alcock, *Inorg. Chem.* **1982**, *21*, 1196–1204; P. G. Antonov, Y. N. Kukushkin, V. G. Shtrele, Y. P. Kostikov, F. K. Egorov, *Zh. Neorg. Khim.* **1982**, *23*, 13–16.
- [5] J. F. Young, *Adv. Inorg. Radiochem.* **1968**, *11*, 91–152; R. D. Cramer, E. L. Jenner, R. V. Jr. Lindsey, U. G. Stolberg, *J. Am. Chem. Soc.* **1963**, *85*, 1691–1692; R. Pietrophano, M. Graziani, U. Belluco, *Inorg. Chem.* **1969**, *8*, 1506–1510; H. van Bekkum, J. van Gogh, G. van Minnen Pathuis, *J. Mol. Catal.* **1967**, *7*, 292–297.
- [6] C. Y. Hsu, M. Orchin, *J. Am. Chem. Soc.* **1975**, *97*, 3553.
- [7] L. Kollár, T. Kégl, J. Bakos, *J. Organomet. Chem.* **1993**, *453*, 155–158.
- [8] L. Wesemann, T. Marx, U. Englert, M. Ruck, *Eur. J. Inorg. Chem.* **1999**, 1563–1566.
- [9] T. Marx, L. Wesemann, S. Dehnen, *Organometallics*, **2000**, *19*, 4653–4657.
- [10] T. Marx, L. Wesemann, *J. Organomet. Chem.* **2000**, *614–615*, 137–143.
- [11] F. Basolo, R. G. Pearson, *Progr. Inorg. Chem.* **1962**, *4*, 381–453.
- [12] a) A. Pidcock, R. E. Richards, L. M. Venanzi, *J. Chem. Soc.* **1966**, *A*, 1707–1710; b) L. M. Venanzi, *Chem. Brit.* **1968**, 162–167; c) T. G. Appleton, H. C. Clark, L. E. Manzer, *Coord. Chem. Rev.* **1973**, *10*, 335–422.
- [13] G. Butler, C. Eaborn, A. Pidcock, *J. Organomet. Chem.* **1979**, *181*, 47–59.
- [14] B. Crociani, R. L. Richards, *J. Organomet. Chem.* **1978**, *144*, 85–93.
- [15] D. F. Christian, H. C. Clark, R. F. Stepanski, *J. Organomet. Chem.* **1976**, *112*, 209–225.
- [16] M. J. Church, M. J. Mays, *J. Chem. Soc. (A)* **1968**, 3074–3078.
- [17] A. Albinati, U. von Gunten, P. S. Pregosin, H. J. Rugg, *J. Organomet. Chem.* **1985**, *295*, 239–256.
- [18] M. Gomez, G. Muller, D. Sainz, J. Sales, X. Solans, *Organometallics*, **1991**, 4036–4045.
- [19] N. H. Dryden, R. J. Puddephatt, S. Roy, J. J. Vittal, *Acta Crystallogr. Sect. C* **1994**, *50*, 533–536.
- [20] a) B. Jovanović, L. Manojlović-Muir, K. W. Muir, *J. Chem. Soc. Dalton Trans.* **1972**, 1178–1181; b) B. Jovanović, L. Manojlović-Muir, *J. Chem. Soc. Dalton Trans.* **1972**, 1176–1178.
- [21] R. Ahlrichs, M. Bär, M. Häser, H. Horn, C. Kölmel, *Chem. Phys. Lett.* **1995**, *242*, 652–657.
- [22] a) R. G. Parr, W. Yang, *Density Functional Theory of Atoms and Molecules*, Oxford University Press, New York **1988**; b) T. Ziegler, *Chem. Rev.* **1991**, *91*, 651–667.
- [23] T. Marx, L. Wesemann, S. Dehnen, *Z. Anorg. Allg. Chem.* **2001**, in press.
- [24] a) K. Eichkorn, O. Treutler, H. Öhm, M. Häser, R. Ahlrichs, *Chem. Phys. Lett.* **1995**, *242*, 652–660; b) K. Eichkorn, F. Weigend, O. Treutler, R. Ahlrichs, *Theor. Chim. Acta* **1997**, *97*, 119–124.
- [25] a) A. D. Becke, *Phys. Rev. A* **1988**, *38*, 3098–3109; b) S. H. Vosko, L. Wilk, M. Nusair, *Can. J. Phys.* **1980**, *58*, 1200–1205; c) J. P. Perdew, *Phys. Rev. B* **1986**, *33*, 8822–8837.
- [26] O. Treutler, R. Ahlrichs, *J. Chem. Phys.*, **1995**, *102*, 346–354.
- [27] A. Schäfer, H. Horn, R. Ahlrichs, *J. Chem. Phys.* **1992**, *97*, 2571–2577.
- [28] M. Dolg, H. Stoll, A. Savin, H. Preuss, *Theor. Chim. Acta*, **1989**, *75*, 173–194.
- [29] R. A. Jacobsen, E. F. Riedel, *Inorg. Chim. Acta* **1970**, *4*, 407–411.
- [30] A. Albinati, P. S. Pregosin, H. Rüttger, *Inorg. Chem.* **1984**, *23*, 3223–3229.
- [31] J. H. Nelson, N. W. Alcock, *Inorg. Chem.* **1982**, *21*, 1196–1200.
- [32] M. Murakami, T. Yoshida, S. Kawanami, Y. Ito, *J. Am. Chem. Soc.* **1995**, *117*, 6408–6409.
- [33] W. A. Herrmann, W. R. Thiel, C. Broßmer, K. Öfele, T. Priermeier, W. Scherer, *J. Organomet. Chem.* **1993**, *461*, 51–60.
- [34] G. W. Parshall, *Inorg. Synth.* **1970**, *12*, 28–29.
- [35] G. Dekker, C. J. Elsevier, K. Vrieze, *Organometallics* **1992**, *11*, 1598–1603.
- [36] a) Fa. Stoe & Cie, X-RED 1.07, Data Reduction for STAD4 and IPDS, Darmstadt **1996**; b) Fa. Stoe, & Cie, X-Shape 1.01, Crystal Optimization for Numerical Absorption Correction, Darmstadt **1996**.
- [37] G. M. Sheldrick, SHELXS 86, Program for Crystal Structure Analysis, Göttingen, Germany **1986**.
- [38] G. M. Sheldrick, SHELXL 97, Program for the Refinement of Crystal Structures, Göttingen **1997**.
- [39] WINGX 1.63: L. J. Farrugia, *J. Appl. Crystallogr.* **1999**, *32*, 837–838.
- [40] SIR 92 - A program for crystal structure solution. A. Altomare, G. Casciarano, C. Giacovazzo and A. Guagliardi, *J. Appl. Crystallogr.* **1993**, *26*, 343–350.
- [41] G. M. Sheldrick, SHELXL 93, Program for the Refinement of Crystal Structures, Göttingen **1993**.
- [42] a) M. N. Burnett, C. K. Johnson, *ORTEP-III*, Report ORNL-6895 **1996**. Oak Ridge National Laboratory, Oak Ridge, Tennessee, U. S. ; b) L. J. Farrugia, *J. Appl. Cryst.* **1997**, *30*, 565.
- [43] Crystallographic data (excluding structure factors) for the structures reported in this paper have been deposited with the Cambridge Crystallographic Data Centre as supplementary publications nos. CCDC-156893 (**7**), CCDC-156895 (**9**), CCDC-156892 (**10-2(CH₃)₂SO**), and CCDC-156894 (**12**). Copies of the data can be obtained free of charge on application to CCDC, 12 Union Road, Cambridge CB2 1EZ, UK (fax: (+44) 1223 336 033; e-mail: deposit@ccdc.cam.ac.uk).

Received: January 30, 2001 [F3038]